SHAKING TABLE TESTS OF LOW-RISE CONCRETE WALLS FOR HOUSING

W.J. Carrillo[1] and S.M. Alcocer[2]

[1] *Ph.D Candidate, Universidad Nacional Autónoma de México, UNAM, México, D.F., & Assistant professor, Universidad Militar Nueva Granada, Bogotá, Colombia*

[2] *Research professor, Instituto de Ingeniería, Universidad Nacional Autónoma de México, UNAM*

Email: wcarrillo@umng.edu.co, salcocerm@ii.unam.mx

ABSTRACT:

Previous low-rise concrete shear walls tested under cyclic loading and designed to fail in shear, reinforced with 50% of the minimum code prescribed wall reinforcement, exhibited comparable displacement ductility to that of walls reinforced with 100% of the minimum steel ratio, thus enabling them to be used in concrete housing. Nevertheless, walls with 50% of the minimum code prescribed wall reinforcement and reinforced with welded wire meshes exhibited limited displacement ductility. This paper presents results of four 1:1.25 scaled concrete walls tested under shaking table excitation aiming at verifying results from quasi-static cyclic loading. Variables studied were the type of concrete (normalweight and cellular), the wall steel ratio (0.125% and 0.25%) and the type of web reinforcement (deformed bars and welded wire meshes). Wall properties were typical of low-rise housing in Mexico. Axial compressive stress, kept constant during the test, was representative of low-rise housing. In the experimental program it was observed that strength and stiffness degradation is more pronounced and displacement capacity is smaller in walls tested under dynamic than under quasi-static cyclic loading. Therefore, loading rate effect plays an important role in the displacement and energy dissipation capacity of low-rise concrete walls.

KEYWORDS: shear walls, reinforced concrete, shaking table test, shear failure, low-rise housing

1. INTRODUCTION

Due to the low seismic demands in low-rise concrete wall housing in Mexico, minimum code prescribed wall reinforcement appears to be excessive for controlling diagonal tension cracking. Taking in to account this concern, a large research program has been underway between the Institute of Engineering of UNAM and CEMEX Group. The experimental program includes quasi-static cyclic test (Sánchez, 2008) and dynamic loading tests (Carrillo, 2008). Cyclic test provided fundamental findings; however, important parameters which depend of the loading rate, like strength and stiffness degradation and energy dissipation capacity, were not possible to investigate thoroughly. Shaking table test were essential not only for verifying static test results but for studying other dynamic characteristics, like fundamental frequencies and damping.

This paper discusses the overall behavior of four 1:1.25 scaled shear walls tested under shaking table excitation. In order to study wall performance under different limit states, from onset of cracking to collapse, specimens were subjected to three earthquake hazard levels. The initial vibration period of the walls was established to agree with ambient vibration tests of typical low-rise housing. The test set-up was purposely designed to carry the additional inertial mass outside the shaking table. Dynamic behavior is compared with results from similar walls tested under quasi-static cyclic loading. Wall performance and cyclic and dynamic hysteretic loops will be presented and analyzed. Results from static and dynamic test are being analyzed to develop a displacement based design approach for safe, economic and comfortable housing.

2. PROTOTYPE ANALYSIS

2.1 Description

The three-dimensional prototype is a two-story reinforced concrete house with shear walls in the two principal directions (see Figure 1.a and 1.b). Typically, wall thickness and clear height are 10 and 240 cm, respectively, and house floor plan area is 62.5 m^2 (5.9 x 10.6 m). Nominal concrete compressive strength is 150 kgf/cm^2. Foundations are strip footings made of reinforced concrete beams (40 cm x 40 cm cross section). In order to know the fundamental vibration period of the prototype, two different identification techniques were used. A non-parametric technique based on conventional spectral analysis of ambient vibration test, and parametric techniques, where a basic mathematic model is established and the necessary structural parameters for producing a good correlation between measured and calculated response are estimated. Although the three-dimensional prototype is a two-story house, mathematic modeling was also carried out in single-story houses. Due to logistic objections, the ambient vibration test was made only in two single-story houses.

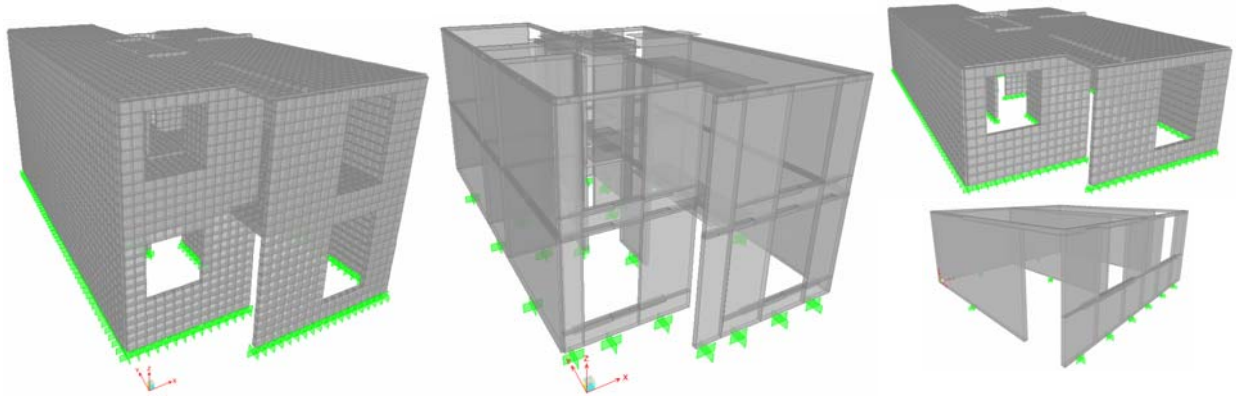

(a) Two stories-FEM (b) Two stories-WCM (c) One story: Type 1-FEM, Type 2-WCM

Figure 1. Mathematic models

2.2 Parametric technique

Two modeling methodologies were used: the wide column method (WCM) and elastic finite element method (FEM) (see Figure 1). In the former, wall properties are concentrated in artificial columns located at the wall centroid (Bazán and Meli, 2004).

2.3 Non-parametric technique

In the ambient vibration test (AVT), using high resolution accelerometers, vibrations generated in the structures for ambient conditions were recorded. This information was useful to understand the structural behavior associated with low amplitudes. Due to the types of the structures, the average power spectrum was used for identifying fundamental vibration frequency (see Figure 2).

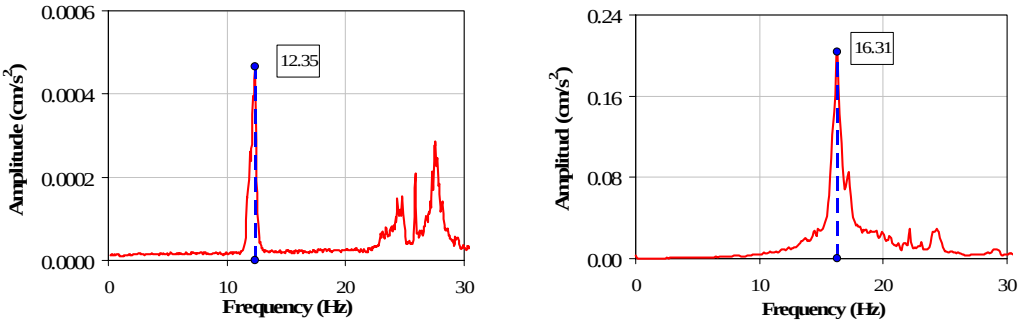

(a) Type 1 (b) Type 2

Figure 2. Average power spectrum for two types of one-story houses

2.4 Isolated wall prototype

Table 1 includes the fundamental vibration period of studied configurations. Although there are a lot of uncertainties in structural modeling (i.e., torsion effects, flexibility of floor diaphragm, construction joints, interaction of non-structural elements, soil-structure interaction), the relations between analytical and measured periods are suitable. Therefore, those two analytical methodologies are acceptable for modeling the elastic behavior of this type of structures. For the two-story house (three-dimensional prototype), the fundamental vibration period is approximately 0.10 s (10 Hz). Thus, for shaking tables test, the initial vibration period of isolated walls (not scaled) was close to this value. Additionally, the geometric and reinforcement characteristics of the models were similar to walls tested under static loading.

Table 1. Fundamental vibration periods of prototype houses

Description		T (s)			T_{AVT} / T_{FEM}	T_{AVT} / T_{WCM}	T_{MEF} / T_{WCM}
Stories	Type	AVT	FEM	WCM			
1	1	0.081	0.059	0.067	1.36	1.21	0.88
	2	0.061	0.049	0.047	1.24	1.30	1.04
2	---	---	0.110	0.121	---	---	0.91

3. EXPERIMENTAL PROGRAM

3.1 Similitude requirements

Due to loading limitations, 1:1.25 scaled models were planed (S_L = 1.25). Because the size of the specimens was very similar to the isolated wall prototypes, a simple similitude law was chosen (Tomazevic y Velechovsky, 1992). In this type of similitude law, the models are built with the same material that the prototype; i.e. materials properties are not changed, only dimension models are altered.

3.2 Geometry and reinforcement

The geometry and layout reinforcement of models are shown in Figure 3. Table 2 and Table 3 show the reinforcement characteristics of walls tested under cyclic loading (prototypes) and shake table excitation (models), respectively. Height, length and thickness of prototypes walls were 240 cm, 240 cm y 10 cm, respectively.

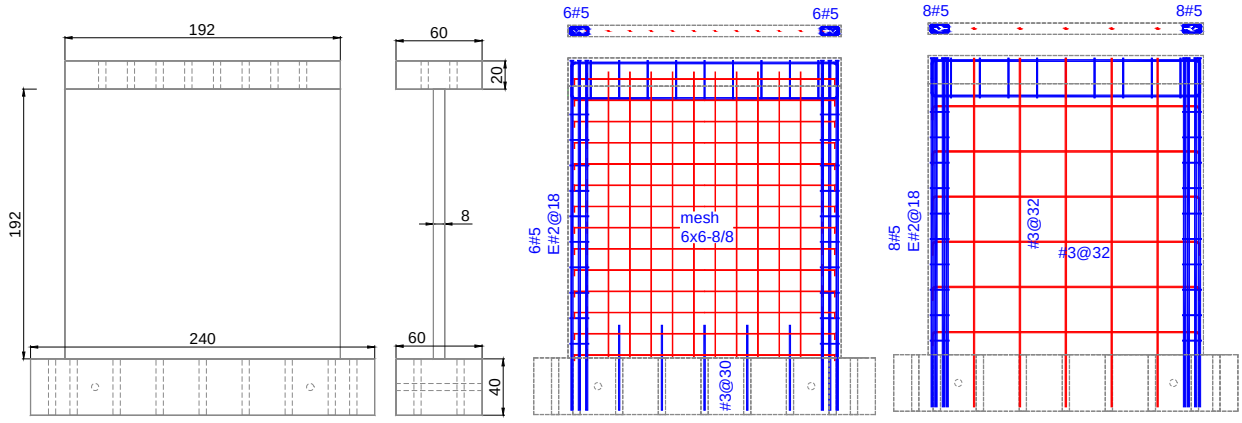

(a) Geometry (dimension in cm) (b) With welded wire mesh (c) With deformed bars

Figure 3. Geometry and layout reinforcement of wall models

Table 2. Reinforcement of walls tested under cyclic loading

No.	Wall	Concrete	Web [1 y 2]	$\rho_v = \rho_h$ (%)	Boundary (flexural) [3]	ρ (%)	Boundary (stirrups) [4]	ρ_s (%)
23	MCN50mC	Normalweight	mesh 6×6-6/6	0.12	6 # 6	0.74	E # 2@15 cm	0.43
10	MCN100C	Normalweight	#3 @ 25 cm	0.28	8 # 6	0.99	E # 2@15 cm	0.43
26	MCC50mC	Cellular	mesh 6×6-6/6	0.12	6 # 6	0.74	E # 2@15 cm	0.43
33	MCC100C	Cellular	#3 @ 25 cm	0.28	6 # 6	0.99	E # 2@15 cm	0.43

Notes:
[1] #3@25: single layer (vertical and horizontal) of No. 3 deformed bars (diameter = 0.95 cm = 3/8 in.) with spacing of 25 cm
[2] 6×6-6/6: single mesh of No. 6 wires (diameter = 0.49 cm) with spacing of 15 cm (~ 6 in.)
[3] 6 # 6: 6 No. 6 deformed bars (diameter = 1.91 cm = 6/8 in.) in each boundary element
[4] E # 2 @15 cm: No. 2 smooth bar stirrups (diameter = 0.64 cm = 2/8 in.) with spacing of 15 cm

Table 3. Reinforcement of walls tested under shake table excitation

No.	Wall	Concrete	Web [1]	$\rho_v = \rho_h$ (%)	Boundary (flexural)	ρ (%)	Boundary (stirrups)	ρ_s (%)
36	MCN50mD	Normalweight	mesh 6×6-8/8	0.11	6 # 5	0.81	E # 2@18 cm	0.43
37	MCN100D	Normalweight	#3 @ 32 cm	0.28	8 # 5	1.08	E # 2@18 cm	0.43
38	MCC50MD	Cellular	mesh 6×6-8/8	0.11	6 # 5	0.81	E # 2@18 cm	0.43
39	MCC100D	Cellular	#3 @ 32 cm	0.28	6 # 5	1.08	E # 2@18 cm	0.43

Notes (similar to Table 2):
[1] 6×6-8/8: single mesh of No. 8 wires (diameter = 0.41 cm) with spacing of 15 cm (~ 6 in.)

3.3 Input motions

In order to study wall performance under different limit states, from onset of cracking to collapse, specimens were subjected to three earthquake hazard levels. An earthquake record from an epicentral region in Mexico (Mw=7.1), was used as a basis for the testing program. The earthquake was recorded in Caleta de Campos station, in January 11, 1997. This record was considered as Green function to simulate larger-magnitude events, i.e. with larger instrumental intensity and duration (Ordaz *et al.*, 1995). Two earthquakes with Mw magnitudes 7.7 and 8.3 were numerically simulated for the strength and ultimate limit states, respectively. Main earthquake characteristics and time histories and spectrums accelerations in the prototypes are presented in Table 4 and Figure 4, respectively.

Table 4. Earthquake characteristics in the prototype houses

Record	Magnitude (M_W)	PGA [1] (g)	Total duration (s)	Intense phase duration (s)	I_A [2] (m/s)	IS_H [3] (m)
CALE71	7.1	0.38	29.52	13.40	2.02	0.50
CALE77	7.7	0.72	36.14	16.30	8.81	0.86
CALE83	8.3	1.30	99.78	40.70	41.63	1.76

Notes:
[1] Peak ground acceleration, [2] Arias intensity, [3] Housner spectral intensity for 5% of damping

Acceleration and time scale factors were applied to these records for the test. Models were tested under progressively more severe earthquake actions, scaled up considering the value of peak acceleration as the reference factor, until the final damage stage was attained. In Table 5, the sequence of input motion used in the tests is described. All tests started with a sine-curve signal (SN), which was used to evaluate the level of friction of the system that transmitted the inertial forces to the models. At the beginning and the end of the tests, a random acceleration signal (white noise – WN) at 10 cm/s^2 (0.01 g) RMS was applied to identify dynamic properties.

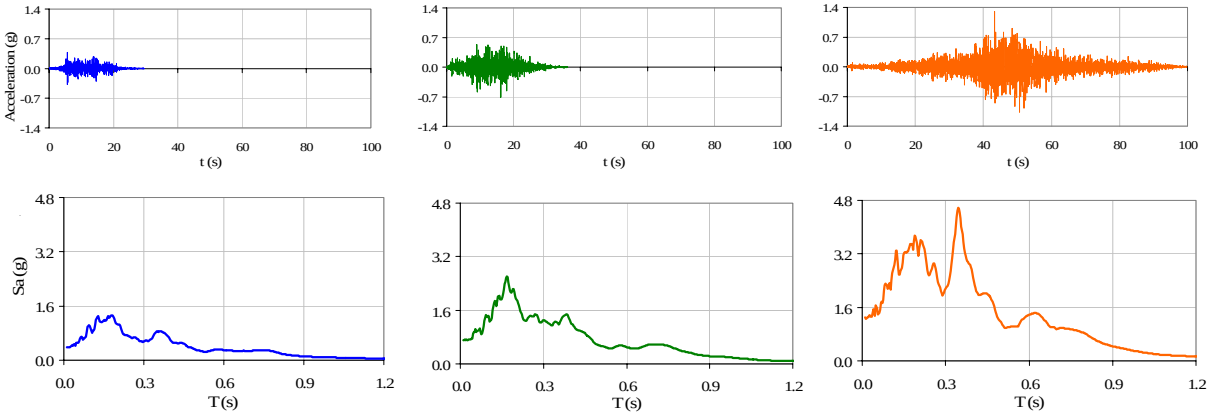

(a) CALE71 (b) CALE77 (C) CALE83

Figure 4. Time histories and spectrums accelerations (ξ = 5%) for the prototype houses

Table 5. Testing stages

Stage	Record	Magnitude (M_W)	PGA (%)	PGA (g)	Total duration (s)
0	SN	---	---	0.01	30
1	WN	---	---	---	120
2	CALE71	---	50	0.24	23.62
3		7.1	100	0.48	
4	CALE77	---	75	0.68	28.91
5		7.7	100	0.90	
6	CALE83	---	75	1.22	79.82
7		8.3	100	1.63	
8	WN	---	---	0.01	120

3.4 Test sep-up

Due to the magnitude of the maximum additional weight (23.9 tf) needed for proper modeling and similitude requirements, it is difficult to simply rest this at the top of individual wall models. Therefore, to avoid the risk of lateral instability of models, an alternative method for supporting the mass and transmitting the inertial forces to the models was required. A mass-carrying system that is allowed to slide horizontally on a supporting structure, located outside the shaking table, was used to carry the mass blocks (lead ingots). The mass blocks were placed in a steel box which is, in turn, supported by a linear motion (LM) guide system with low friction. The LM guide system has two components: LM rail and LM block. According to the amount of the additional weight, two rails with three blocks each were used. For connecting the inertial mass and the models a connection beam with pinned ends (free plane rotations) and a load beam were used. A load cell was placed in the connection beam to measure the partial load on specimens (see Figure 5).

Prior to each test, a low frequency (T = 2 s) sine curve signal was applied to the platform. Such input motion, applied at relatively low velocity, induced negligible response of the models. Therefore, any source of resistance to the applied motion could originate only from friction being developed in the LM guide system. In this manner, the level of friction could be quantified. Ideally, the friction level of the system should be close to zero and fortunately, it was the case. The level of friction was very low (close to 1.0%). Further, the test sep-up allowed for a smooth response of the models, because of the system did not introduce significant damping in the response.

An axial compressive stress of 2.5 kg/cm^2, which corresponds to roughly 2% of the nominal concrete compressive strength, was applied at the top of the walls. Finite element models of two-story houses (see Figure 1.a) were used to determine this value for service loads, and therefore it is considered representative of low-rise

housing. The axial load, kept constant during the test, was achieved through the weight of the load and connection beam and with lead ingots bolted to the load beam (see Figure 5).

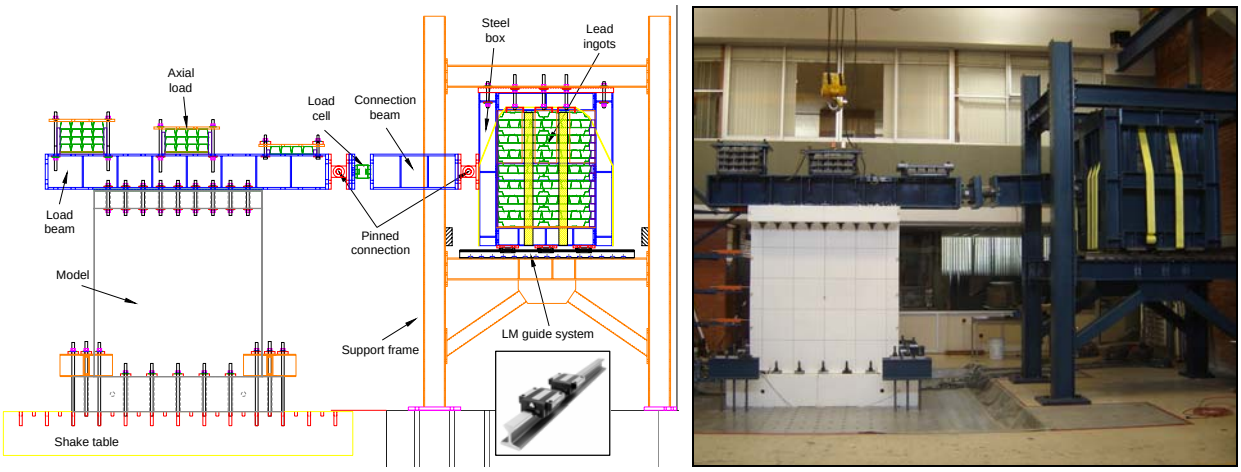

Figure 5. Test sep-up

3.5 Instrumentation

Models were instrumented internally and externally. Internal instrumentation was necessary to get information of the local response using strain-gages glued to the steel reinforcement. External instrumentation was used to know the global response using displacement, acceleration and load transducers. Also, an optical displacement measurement system (with Light Emitting Diodes - LED's) was used. In the test, 41 internal strain-gages and 36 external transducers were used (see Figure 6).

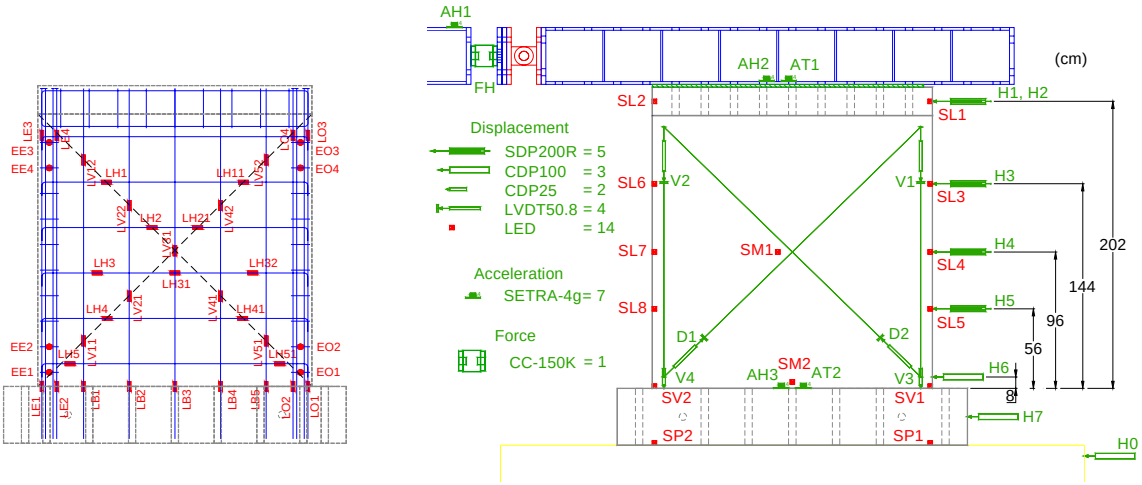

(a) Internal (with deformed bars) (b) External

Figure 6. Instrumentation of wall models

3.6 Mechanicals properties of materials

Average mechanical properties of concrete and steel reinforcement are presented in Table 6 and Table 7, respectively. For concrete, these properties were obtained close to test models date. Compressive strength of concrete walls 23, 10, 26 and 33 tested under cyclic loading was 204, 178, 265 and 53 kg/cm^2, respectively (see Table 2).

Table 6. Mechanical properties of concrete

Mechanical property	Wall	
	MCN50mD (36) MCN100D (37)	MCC50mD (38) MCC100D (39)
Type	Normalweight	Cellular
Age at testing (days)	252	246
Compressive strength, f_c (kgf/cm^2)	252	214
Elastic modulus, E_c (kgf/cm^2)	150424	93228
Poisson's ratio, ν	0.16	0.16
Flexural strength, f_t (kgf/cm^2)	38.2	33.5
Tensile strength, f_r (kgf/cm^2)	21.3	14.7
Specific weight, γ (kgf/m^3)	2073	1712

Table 7. Mechanical properties of steel reinforcement

Diameter, d_b		Type bar	f_y (kgf/cm^2)	ε_y	E_s (kgf/cm^2)	ε_{sh}	E_{sh} (kgf/cm^2)	f_{su} (kgf/cm^2)	ε_{su}	*Elong.* (%)
in.	cm									
5/8	1.59	Deformed	4185	0.0022	1872378	0.0119	100238	6689	0.0786	12.2
3/8	0.95	Deformed	4434	0.0022	2009328	0.0130	107116	6722	0.0730	10.1
1/4	0.64	Smooth	2785	0.0019	1477495	0.0253	27801	3953	0.1426	19.2
---	0.411	Wire	6423	0.0036	2470138	---	---	7002	0.0082	1.9

Notes:
f_y = yield strength, f_{su} = maximum strength, ε_y = yield strain, ε_{sh} = strain hardening, ε_{su} = strain at maximum strength
E_s = elastic modulus, E_{sh} = strain hardening modulus, *Elong.* = elongation

4. TEST RESULTS

4.1 Vibration frequencies

Determinations of natural frequencies of a reinforced concrete structural system are of a vital importance to earthquake-resistant design. Models frequencies were achieved using the transfer function between accelerations measured at the shaking table and the load beam. As expected, a key characteristic of test specimens was the change in measured frequency with the reduction in stiffness caused by the seismic excitation. Figure 7 shows the change in the fundamental frequency with the drift ratio for normalweight concrete walls. Achieved initial frequency was lower that target one (12.5 Hz, 0.08 s) because of premature cracking. These cracks may have been caused as the specimens were prepared for test and for shrinkage concrete. The figure shows that small amounts of damage significantly reduced the fundamental frequency of each specimen. Trends for cellular concrete walls were similar.

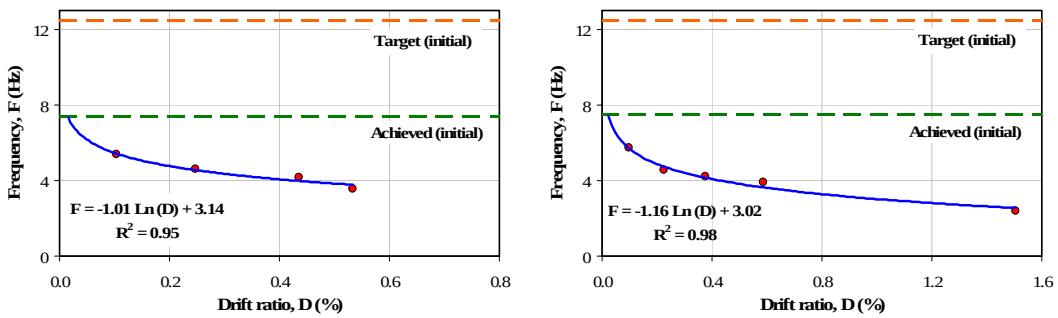

(a) MCN50mD-36 (b) MCN100D-37

Figure 7. Vibration frequencies

4.2 Crack patterns and failure mode

As mentioned earlier, prior to testing, walls exhibited premature shrinkage cracking. Nevertheless, these cracks only affected wall initial stiffness. Walls reinforced with welded wire mesh and with 50% of the minimum code prescribed steel ratio exhibited diagonal tension failure (see Figure 8.a-b). Failure was brittle because of the limited deformation capacity of the wire mesh. In contrast, walls reinforced with deformed bars and with 100% of the minimum steel ratio, a more ductile, diagonal compression failures were observed (see Figure 8.c-d). Similar walls tested under quasi-static cyclic loading exhibited comparable failure mode and performance.

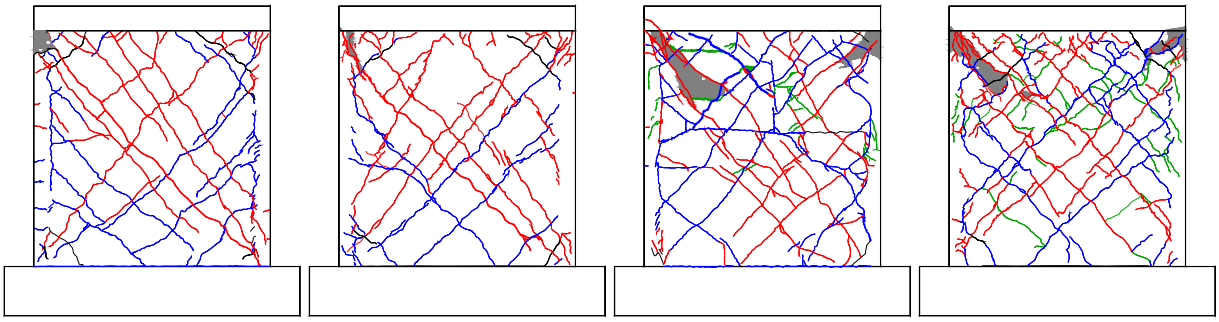

(a) MCN50mD-36 (b) MCC50mD-38 (c) MCN100D-37 (d) MCC100D-39

Figure 8. Final cracks patterns

4.3 Hysteretic curves – Comparison with quasi-static cyclic loading tests

To assess the overall performance of walls, the hysteretic curves in terms of the shear stress (or lateral force) and lateral drift are shown on the left side in Figure 9. The lateral force was calculated from measured force in load cell and extra inertial force generated between load cell and the specimens (see Figure 5). For comparison purposes, the lateral force was affected with the theoretic scale factor ($S_F = S_L^2$). On the right side of the figure, results of similar walls tested under quasi-static cyclic loading are shown. Most important results are summarized in Table 8.

Table 8. Measured response characteristics - Dynamic and static test

Characteristic	MCN50m		MCC50m		MCN100		MCC100	
	D	S	D	S	D	S	D	S
Lateral force (Max.), tnf	37.50	34.47	38.84	41.77	44.07	48.10	40.53	36.87
Shear stress (Max.), kgf/cm^2	15.04	14.00	15.86	17.32	17.49	19.87	16.62	15.70
Drift ratio (Max. shear stress), %	0.42	0.58	0.55	0.60	0.54	0.62	0.48	0.79
Drift ratio (Max), %	0.57	0.58	0.68	0.66	1.58	1.84	1.53	1.79

Observed deformation capacity was smaller in walls tested under dynamic loading. Only in wall MCC50m it was a slightly larger. This finding is more remarkable for the drift ratio associated with the maximum shear stress (see Table 8). In walls tested under static loading and reinforced with deformed bars, strength degradation takes place at drifts much larger than those associated to maximum shear strength. Additionally, degradation rate is very low. In contrast, strength degradation in dynamic test began as soon the maximum shear stress is reached. Also, degradation rate was more pronounced. Almost certainly, differences in behavior are related to the loading rate effect. However, in walls reinforced with welded wire mesh, in which the inelastic portion of the stress-strain curve is almost nonexistent, the effect is not so apparent. Because strength and stiffness degradation have an important role in the energy dissipation capacity of structures, deformation results obtained for shear walls tested under quasi-static cyclic test are only a first approximation of the true behavior of these elements under seismic loading.

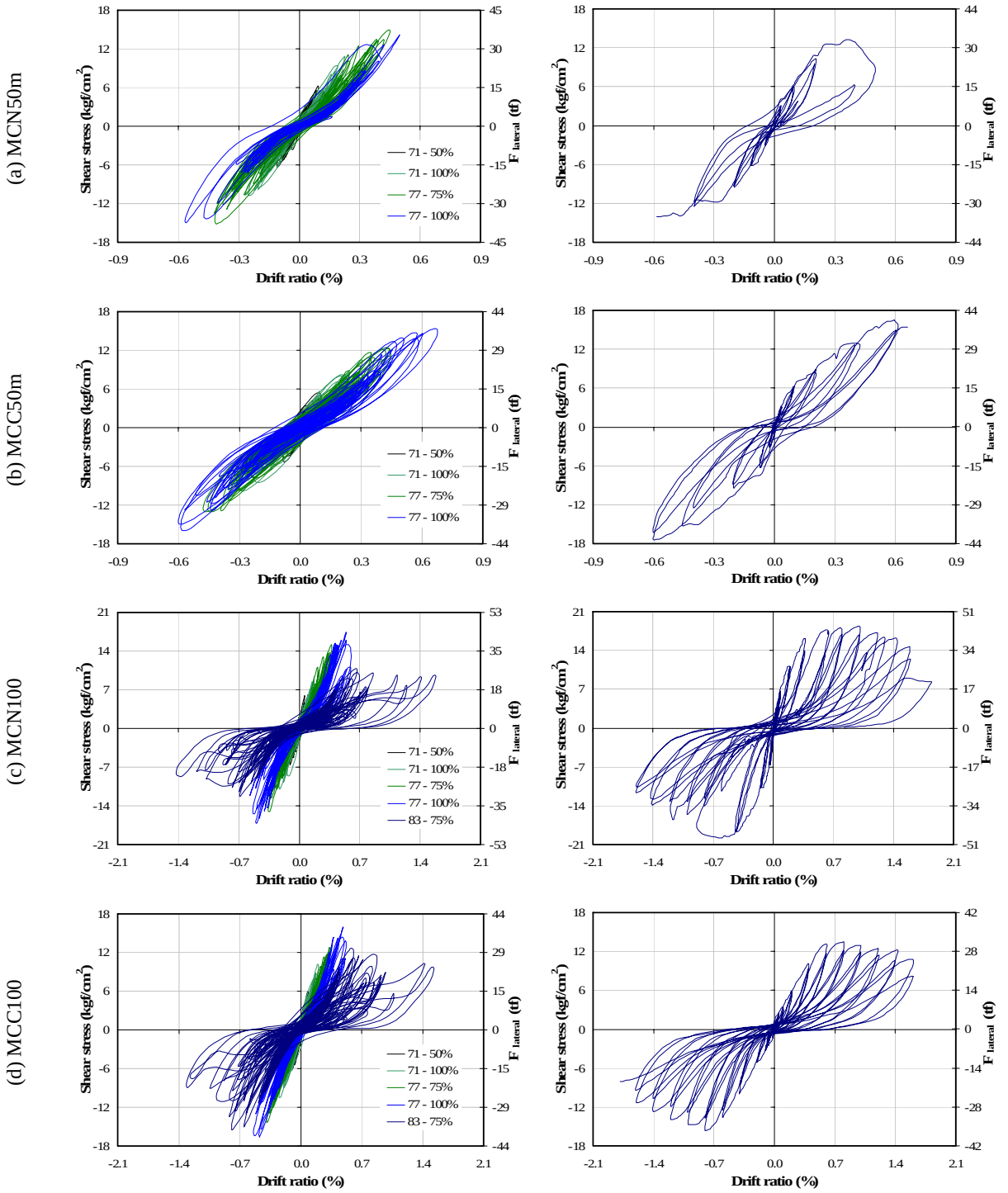

Figure 9. Hysteretic curves

It is important to see in Table 8 that maximum shear stress of walls tested under dynamic loading and reinforced with 50% of the minimum code prescribed wall reinforcement was comparable to those walls reinforced with 100% of the minimum amount. Also, behavior of normalweight and cellular concrete walls was, in general similar.

4.4 Deformation analysis

An attempt has been made to determine the effect of each mode of deformation on the total displacement of the wall specimens by separately calculating the shear deformation in the web, the flexural deformation and the horizontal sliding at the base. It was possible to evaluate the total error in the estimation of the contribution (discrepancy between measured and calculated total displacement). This error never exceeded 10% and was distributed proportionally among the three deformation components. Figure 10 shows the contribution of each deformation mode to the total drift ratio of walls, plotted for each record and for various ductility levels. The displacement ductility factor was estimated by dividing the maximum displacement achieved on each record by a conventional yield displacement, corresponding to the development of 75% of the maximum strength.

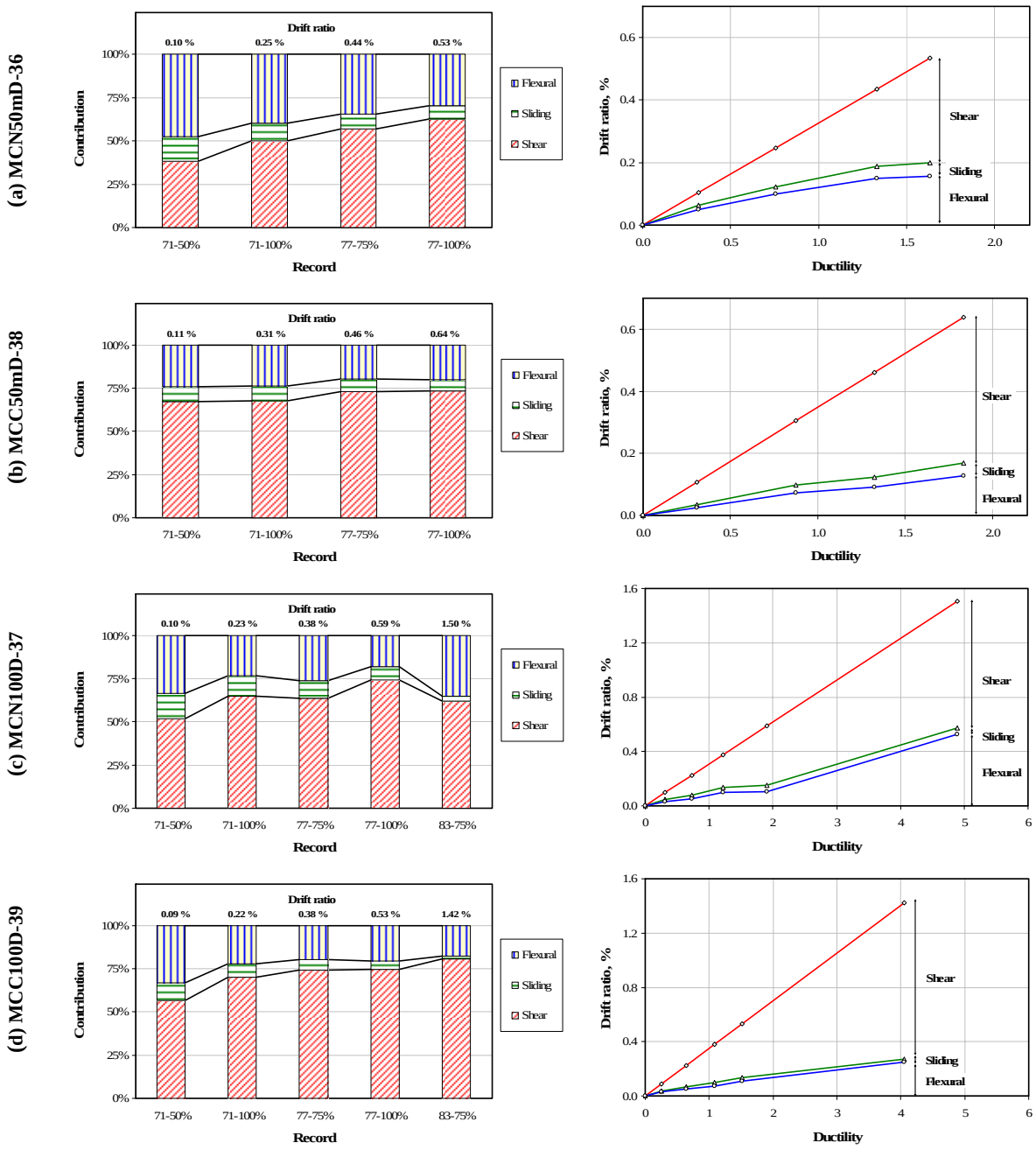

Figure 10. Contribution of various deformation modes to drift ratio

It is clear from Figure 10 that the behavior of the specimens was always controlled for shear mechanism (web shear and sliding shear) and that relative contribution of each mode varied significantly with the ductility level. Initially, contribution of flexural deformations played an important role in the response; however, it decreased at higher drift demands. Note that the sliding shear component accounted for about 15% initially, but decreased to 8% close to failure. Ductility capacities of walls with normalweight (Figure 10.a and Figure 10.b) and cellular concrete (Figure 10.c and Figure 10.d) were similar. Although walls with deformed bars were reinforced with 100% of the minimum code prescribed steel ratio, and walls with welded wire mesh had 50% of the minimum amount, ductility capacity of the former was almost three times of the latter.

5. FINAL REMARKS

Based on the partial data analysis carried out so far, it may be concluded that shaking table test was useful to compare results from quasi-static cyclic tests. Considering measured frequencies, linear elastic analysis based on "uncracked" properties are deemed not realistic and may be unreasonably conservative particularly for lightly reinforced concrete walls. The effect of loading rate plays an important role on the deformation capacity, and strength and stiffness degradation of low-rise concrete walls. As a result, energy dissipation capacity calculated from quasi-static cyclic test could be overestimated. Walls reinforced with 50% of the minimum code prescribed wall steel ratio and using welded wire meshes, exhibited comparable shear stress capacity to that of walls reinforced with 100% of the minimum amount, thus enabling them to be used in concrete housing where the displacement demands are not a main concern.

REFERENCES

Alcocer S., Sánchez A., Uribe R. and Ponce A. (2006). Behavior of concrete walls for economic housing. 8th U.S. National Conference of Earthquake *Engineering*, San Francisco, California. Paper 1834

Arias A. (1970). A measure of earthquake intensity. In: Seismic design for nuclear power plants. Editor: R. J. Hansen, MIT Pres, 438-483.

Bazán E. and Meli R. (2004). Diseño sísmico de edificios. Limusa S. A., Mexico.

Carrillo J. (2008). Evaluación del comportamiento al cortante de muros de concreto para vivienda por medio de ensayes dinámicos. Ph.D thesis (In process). Universidad Nacional Autónoma de México.

Flores L., Alcocer S., Carrillo J., Sánchez A., Uribe R. and Ponce A. (2007). Ensaye de muros de concreto con diferente relación de aspecto y bajas cuantías de refuerzo, para uso en vivienda. XVI National Congress on Earthquake Engineering, Ixtapa-Zihuatanejo, Guerrero, Mexico. Topic XI, Paper 2.

Housner G. (1959). Behavior of structures during earthquakes. *Journal of the Engineering Mechanics Division – ASCE* **85:EM4**, 109-129.

Muriá D. and González R. (1995). Propiedades dinámicas de edificios de la ciudad de México. *Revista de Ingeniería Sísmica* **51**, 25-45. México.

Ordaz M., Arboleda J. and Singh S. (1995). A Scheme of Random Summation of an Empirical Green's Function to Estimate Ground Motions from Future Large Earthquakes. *Bulletin of the Seismological Society of America* **85:6**, 1635-1647.

Pinho R. (2000). Shaking table testing of RC walls. *Journal of Earthquake Technology* **37:4**, 119-142.

Sánchez A. (2008). Comportamiento sísmico de viviendas construidas con muros de concreto. Ph.D thesis (In process). Universidad Nacional Autónoma de México.

Tomazevic M. and Velechovsky T. (1992). Some aspects of testing small-scale masonry building model on simple earthquake simulator. *Journal of Earthquake Engineering and structural Dynamics* **21:11**, 945-963.